IOPscience iopscience.iop.org

Home Search Collections Journals About Contact us My IOPscience

Cu nuclear magnetic resonance study of the magnetic structure in $NdCu_2$

This article has been downloaded from IOPscience. Please scroll down to see the full text article.

1995 J. Phys.: Condens. Matter 7 6885

(http://iopscience.iop.org/0953-8984/7/34/012)

View the table of contents for this issue, or go to the journal homepage for more

Download details:
IP Address: 171.66.16.151
The article was downloaded on 12/05/2010 at 22:00

Please note that terms and conditions apply.

J. Phys.: Condens. Matter 7 (1995) 6885–6897. Printed in the UK

Cu nuclear magnetic resonance study of the magnetic structure in $NdCu_2$

H Takahashi†, H Nakamura†, M Shiga† and E Gratz‡

† Department of Materials Science and Engineering, Kyoto University, Kyoto 606-01, Japan
‡ Institut für Experimentalphysik, Technische Universität Wien, A-1040 Wien, Austria

Received 25 October 1994, in final form 16 May 1995

Abstract. In order to investigate the magnetic interaction in the paramagnetic and the antiferromagnetic state of $NdCu_2$, we measured the Cu nuclear magnetic resonance (NMR). In $NdCu_2$ an antiferromagnetic long-range order exists below $T_N = 6.5$ K and a change of the spin structure around 4.1 K has been reported. For the paramagnetic state, we have deduced the hyperfine coupling constant and the electrostatic parameters at the Cu sites, such as the principal axis of the electric field gradient, the nuclear quadrupole frequency and the anisotropy parameter. The nuclear quadrupole resonance line splits into several lines in the ordered state due to the onset of the hyperfine field, which can be calculated assuming two different magnetic Cu sites. We discuss the consistency between these NMR results and the magnetic structure proposed by recently performed neutron diffraction experiments.

1. Introduction

The intermetallic compounds RCu_2 (R = rare earth) show the orthorhombic $CeCu_2$-type structure. Due to the low symmetry of this structure, the magnetic properties are highly anisotropic. At low temperatures, all of these compounds (except R = Y, Pr, Yb, Lu) exhibit an antiferromagnetic spin arrangement, which is in general very sensitive to an applied field. The magnetic structures of most of these compounds have been investigated by neutron diffraction experiments (see, for example, Lebech *et al* 1987). Decades ago the magnetization of $NdCu_2$ was studied (Sherwood *et al* 1964, Hashimoto *et al* 1979) and has recently been reinvestigated in more detail (Gratz *et al* 1991, 1993, Svoboda *et al* 1992, Bozukov *et al* 1992). In zero external field, $NdCu_2$ orders at $T_N = 6.5$ K and exhibits a magnetic instability at $T_R = 4.1$ K. Using neutron diffraction measurements, recently the magnetic structures of both the low-temperature and the high-temperature phase were found to be long period modulated (Arons *et al* 1994, Loewenhaupt *et al* 1995). From these experiments it follows that the magnetic structure between 6.5 K and 4.1 K can be described by an incommensurate wave vector $\tau^* = (0.62, 0.044, 0)$, and transfers into a commensurate spin arrangement with $\tau = (0.6, 0, 0)$ below 4.1 K. From single-crystal measurements, Loewenhaupt *et al* (1995) confirmed the completely squared-up arrangement of the spins along the *b*-direction for the low-temperature state towards zero temperature.

In the present investigation, we approach the magnetic structure by studying the Cu nuclear magnetic resonance (NMR) which gives microscopic information on the local field at the Cu sites. Unfortunately, we could not observe the NMR signal for the incommensurate high-temperature phase (4.1 K $< T <$ 6.5 K) presumably due to the short nuclear spin relaxation time; however a well resolved spectrum for the low-temperature phase

0953-8984/95/346885+13$19.50 © 1995 IOP Publishing Ltd

($0 < T \leqslant 4.1$ K) could be obtained. It is usually a tough task to analyse NMR results of modulated magnetic structures because of the complex local field distribution. This article demonstrates a successful NMR study for determining the magnetic structure in $NdCu_2$. To our knowledge this is the first report on an NMR study in an RCu_2 system.

2. Experimental details

Polycrystalline samples were prepared by induction melting in a protective argon atmosphere. For NMR experiments, the sample was crushed into powder with grain size smaller than 50 μm. The Cu NMR was measured using a phase-coherent-type pulsed spectrometer in the temperature range between 1.4 and 200 K. Since Cu has two isotopes, ^{63}Cu (nuclear spin $I = \frac{3}{2}$) and ^{65}Cu ($I = \frac{3}{2}$), with the natural abundance 69% and 31%, respectively, we always expect a pair of resonances of ^{63}Cu and ^{65}Cu with the intensity ratio about 7:3. For the gyromagnetic ratios of ^{63}Cu and ^{65}Cu, the values $^{63}\gamma/2\pi = 1.1285$ MHz kOe^{-1} and $^{65}\gamma/2\pi = 1.2089$ MHz kOe^{-1} were used.

Details of the structural data can be summarized as follows. $NdCu_2$ forms the orthorhombic $CeCu_2$-type structure with the space group D_{2h}^{28} (*Imma*). Nd and Cu atoms occupy the 4e and 8h sites, respectively. The positions of the Nd and Cu atoms inside the unit cell are given by

$$4\text{e site}(0, \tfrac{1}{4}, x), (0, \tfrac{3}{4}, -x)$$

$$8\text{h site}(0, y, z), (0, -y, -z), (0, \tfrac{1}{2} + y, -z), (0, \tfrac{1}{2} - y, z).$$

Gratz *et al* (1991) reported that based on a Rietveld analysis the x-ray diffraction pattern can be reproduced with the parameters $x = 0.5383$, $y = 0.0506$ and $z = 0.1659$. Since the symmetry on the 8h sites is low (m) the Cu ions on these sites experience a finite electric field gradient (EFG), $eq = V_{ZZ}$, with an anisotropy parameter, $\eta = (V_{XX} - V_{YY})/V_{ZZ}$, where V_{XX}, V_{YY} and V_{ZZ} are the diagonal components of the EFG tensor at the Cu nuclear sites. The Cu atom at the origin is firstly surrounded by four Cu atoms and secondly by six Nd atoms at a distance of about 3.0–3.2 Å, which can be considered as effective nearest-neighbour magnetic atoms.

3. Experimental results

3.1. The paramagnetic state

3.1.1. The NQR spectrum. Figure 1 shows the NQR spectrum at 52 K. This resonance line corresponds to the $m = \pm\frac{1}{2} \leftrightarrow \pm\frac{3}{2}$ transitions for ^{63}Cu caused by the electric quadrupolar interaction, where m denotes the magnetic quantum number of the nuclear spin. We obtained the spectrum for ^{63}Cu by accumulating the spin echo signal several hundred times because the intensity was very weak due to the very short spin echo decay time, which may be due to a very short nuclear spin–lattice relaxation time, T_1. The full curve in figure 1 indicates the best fit of a Gaussian function to the experimental data with a resonance frequency $^{63}\nu_{NQR} = 8.88$ MHz and a linewidth $\Delta\nu = 230$ kHz. The broken line indicates where the NQR signal for ^{65}Cu is expected; however it seems that the signal to noise ratio is too poor for the line to be observed. For the calculation quadrupole moments $^{63}Q = -0.211$ barns and $^{65}Q = -0.195$ barns have been used.

For the nuclear spin $I = \frac{3}{2}$, the NQR resonance frequency, ν_{NQR}, is given by

$$\nu_{NQR} = \tfrac{1}{2}(e^2qQ/h)\sqrt{1 + \eta^2/3} \equiv \nu_Q\sqrt{1 + \eta^2/3} \tag{1}$$

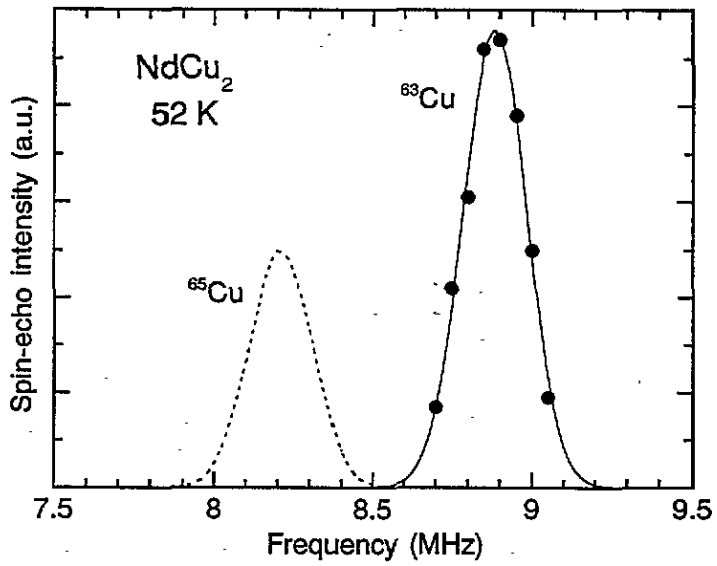

Figure 1. The Cu NMR spectrum of $NdCu_2$ at 52 K, which was obtained by accumulating the spin echo signal several hundred times. The solid line shows the fit of a Gaussian function to the data of ^{63}Cu using a resonance frequency $^{63}\nu_{NQR} = 8.88$ MHz and a half width $\Delta\nu = 230$ kHz. The broken line indicates the expected spectrum for ^{65}Cu, which could not be observed because of the poor signal to noise ratio.

where ν_Q is the pure quadruple frequency and η is the anisotropy parameter. Generally, η and ν_Q cannot be determined independently from the NQR frequency for the nuclear spin $I = \frac{3}{2}$.

3.1.2. The field-swept powder pattern spectrum. In order to determine η, we measured the field-swept NMR spectrum of a powdered sample fixed with paraffin. The spectrum measured at 200 K is shown in figure 2(a). The first-order satellite pair and the central line broadened by the second-order quadrupole effect and the magnetic anisotropy were observed for both ^{63}Cu and ^{65}Cu. The small sharp signals indicated by the open triangles obviously correspond to the Knight shift of pure metallic Cu. The reason for the pure Cu signal seems to be connected with a fractional oxidation of Nd and Cu on the surface of the sample.

Generally, the resonance frequency shift from the true central resonance $\nu_0 (= \gamma H_{hf}$, where H_{hf} is the hyperfine field) of the transition between m and $m-1$ levels is given by

$$\nu_m = \tfrac{1}{2}(m - \tfrac{1}{2})\nu_Q(3\cos^2\theta - 1 - \eta\sin^2\theta\cos 2\phi) \tag{2}$$

within the first-order perturbation of the electric quadrupole interaction. In the case of $\eta = 0$, the satellite pair shows a singularity (divergence) at $\theta = 90°$, where θ is the angle between the external field and the principal axis (Z axis) of the EFG. Assuming a finite η value, the divergence at $\theta = 90°$ shows a structure that means it is separated into two singular edges with $\phi = 0°$ and 90°, where ϕ is the azimuthal angle. These singular points appear at

$$\begin{aligned} \nu_m(\theta = 90°, \phi = 0°) &= -\tfrac{1}{2}(m - \tfrac{1}{2})\nu_Q(1 + \eta) \\ \nu_m(\theta = 90°, \phi = 90°) &= -\tfrac{1}{2}(m - \tfrac{1}{2})\nu_Q(1 - \eta). \end{aligned} \tag{3}$$

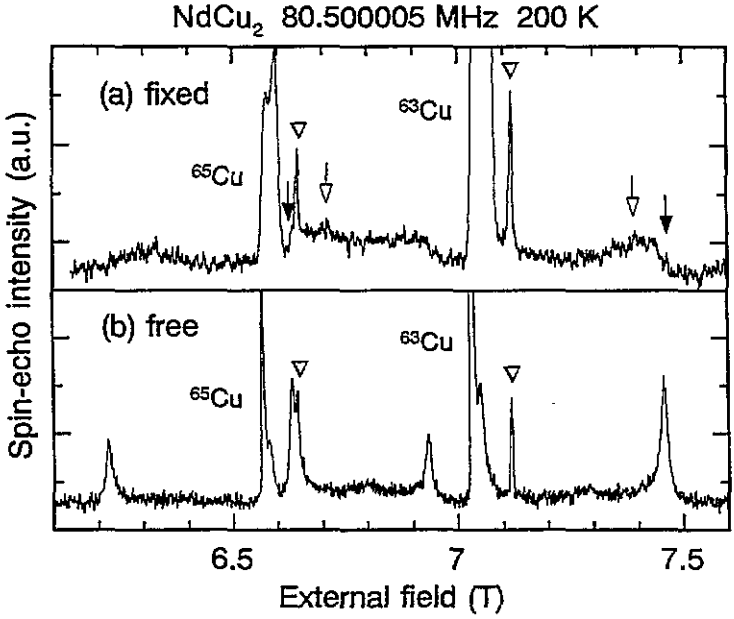

Figure 2. Field-swept NMR spectra of $NdCu_2$ measured at 80.500 005 MHz and 200 K. Triangles indicate pure Cu impurity signals with the metallic Knight shift. (a) The powder pattern spectrum measured for a fixed powder sample. Arrows indicate singular edges of first-order satellite pairs for ^{63}Cu corresponding to $\theta = 90°$ and $\phi = 0°$ (closed) or 90° (open). (b) The oriented powder spectrum measured for a free-powder sample. Under this condition, the a axis of the crystals are parallel to the external field. The satellite pairs are located at the position $\pm 1/2\nu_Q(1+\eta)$ away from the true centre of the resonance.

Hence, the subtraction reveals

$$\nu_m(\theta = 90°, \phi = 90°) - \nu_m(\theta = 90°, \phi = 0°) = (m - \tfrac{1}{2})\eta\nu_Q. \tag{4}$$

The central point is given by

$$\tfrac{1}{2}\{\nu_m(\theta = 90°, \phi = 90°) + \nu_m(\theta = 90°, \phi = 0°)\} = \tfrac{1}{2}(m - \tfrac{1}{2})\nu_Q. \tag{5}$$

Using (4) and (5) we are able to determine η and ν_Q separately. Analysing the powder pattern at 200 K in figure 2(a), we obtain

$$\eta = 0.10 \pm 0.01$$
$$^{63}\nu_Q = 8.73 \pm 0.10 \text{ MHz}$$

for ^{63}Cu. Under the assumption that η is temperature independent and using $^{63}\nu_{NQR} = 8.88$ MHz (at 52 K obtained from NQR experiments) we are able to estimate $^{63}\nu_Q = 8.86$ MHz for 52 K, which is slightly larger than the value for 200 K. This difference can be ascribed to the temperature dependence of ν_Q associated with the thermal expansion.

3.1.3. The field-swept oriented powder spectrum. For the discussion of the magnetic structure based on the local field at the nuclear sites, it is necessary to know the direction of the principal axes of the EFG tensor. In order to determine the relation between the principal axes of the EFG and the crystal axes, we measured the field-swept spectrum for the free powder sample. Figure 2(b) shows the spectrum measured at 200 K on powder

oriented in a large external field. The orientation is possible due to the large anisotropy of the magnetic susceptibility. Svoboda *et al* (1992) reported that the easy magnetization axis below 14 K is the *b* axis, but there is a change to the *a* axis above 14 K. Therefore, at 200 K, the *a* axis of the crystal is expected to be parallel to the field provided that the particles are small enough to be regarded as single crystals. In figure 2(b), well resolved satellite pairs and sharp central lines were found for both ^{63}Cu and ^{65}Cu.

In the following we determine the direction of the principal axis (Z axis) of the EFG tensor. Capital letters will be used to denote the coordinate system of the EFG. For simplicity, we only consider the cases where the easy magnetization axis (*a* axis) coincides with either the X, Y or Z axis, thus three possibilities will be considered: (i) *a* axis$\parallel$ Z axis, i.e., $\theta = 0°$; (ii) *a* axis$\parallel$ Y axis, i.e. $\theta = 90°$, $\phi = 90°$ and (iii) *a* axis$\parallel$ X axis, i.e. $\theta = 90°$, $\phi = 0°$. Using (3) and taking into account that the satellite pair is observable at $\pm\frac{1}{2}\nu_Q(1+\eta)$, which coincides with the outer edge of the first-order satellites in the powder spectrum, only case (iii) is in accordance with the experimental result. Therefore, we can conclude that the Z axis is perpendicular to the *a* axis. Although we cannot determine the Z axis direction in the *bc* plane, it is plausible that the Z axis is parallel to the *b* axis when taking into account other experimental results in the magnetically ordered state, which will be discussed below.

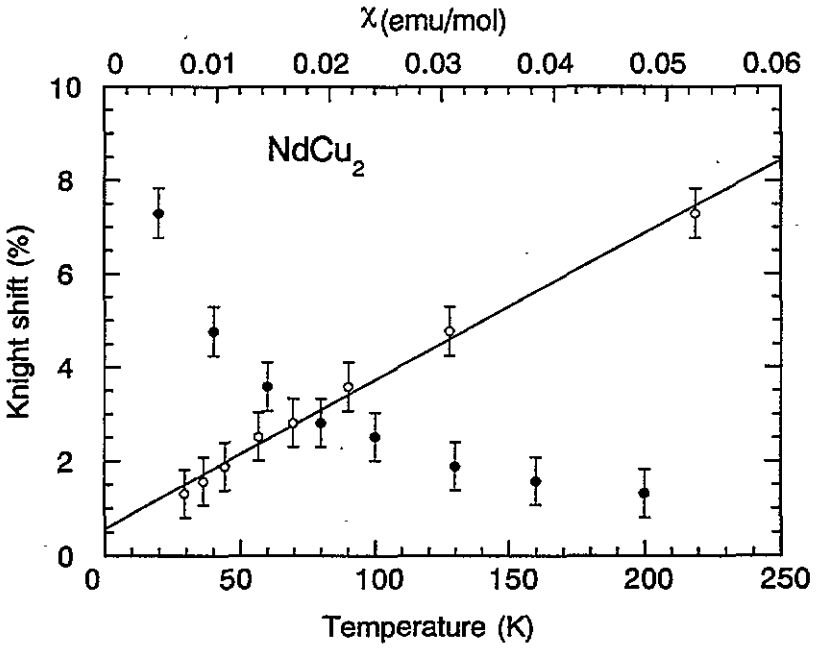

Figure 3. Closed circles, the temperature dependence of the Knight shift ($H \parallel a$ axis) of $NdCu_2$ between 20 K and 200 K, which was measured for an oriented powder sample at 90.300 005 MHz. Open circles, the Knight shift–susceptibility plot of $NdCu_2$ with temperature as an implicit parameter. The hyperfine coupling constant was estimated as $A = 7.34$ kOe μ_B^{-1} from the slope of the straight line.

3.1.4. The Knight shift. The central line of the oriented powder spectrum at 200 K (figure 2(b)) is asymmetric due to the combined effect of the second-order quadrupole splitting and the anisotropic Knight shift and/or the imperfect orientation. In general, very

complicated procedures are necessary to estimate the precise Knight shift for the low-symmetry nuclear site affected by the quadrupole interaction. Here, for simplicity, we make a crude estimation of the Knight shift. If η and the anisotropy of the Knight shift are small, the resonance field of the main peak in the oriented powder spectrum gives approximately the isotropic Knight shift for $\theta = 90°$ and $\phi = 0°$ ($H \parallel a$ axis). Figure 3 (closed circles) shows the temperature dependence of the Knight shift between 20 K and 200 K estimated from the resonance field of the main peak. The above simplification seems to be justified because the values of the Knight shift are markedly large, of the order of several per cent, which is much larger than the anisotropic shift estimated roughly from the width of the central line. Note that the calculated classical dipole field is of the order of 100 Oe μ_B^{-1}. The Knight shift increases rapidly with decreasing temperature, reflecting a Curie–Weiss behaviour of the susceptibility. In figure 3, the Knight shift versus the susceptibility is also plotted with temperature as an implicit parameter (open circles). The susceptibility data are taken from the article by Gratz *et al* (1991) although they were measured for a polycrystalline sample. As seen from figure 3, the Knight shift is proportional to the susceptibility. The slope of this line gives a unique hyperfine coupling constant:

$$A = 7.34 \text{ kOe } \mu_B^{-1}.$$

This is roughly recognized as the isotropic component of the hyperfine coupling constant in the condition $H \parallel a$ axis.

3.2. The magnetically ordered state

3.2.1. The field-swept spectrum in high fields. We measured a field-swept spectrum for the free powder sample at 1.4 K (commensurate antiferromagnetic phase). The line shape at about 80 MHz is shown as an example in figure 4. A superposed spectrum consisting of central lines and satellite pairs for both ^{63}Cu and ^{65}Cu was observed. At 1.4 K, the spins are ferromagnetically aligned along the b axis in fields above about 3 T. Thus the b axis of the sample is oriented along the external field. Therefore, the resonance shift of the central line gives approximately the hyperfine field at the Cu site assuming that the b axis is the local principal axis. The resonance fields of the field-swept spectra measured at some fixed frequencies are presented in figure 5. The data points are on a straight line whose intersection of the frequency axis gives the hyperfine field in the ferromagnetic state. The intersection of the straight line ($\sim$ 17 MHz) corresponds to an internal field of $\sim$ 15 kOe. According to neutron diffraction measurements in the antiferromagnetic state, the ordered moment is 1.78μ_B/Nd (Loewenhaupt *et al* 1995). Using this value and applying the hyperfine coupling constant estimated from the K–χ plot in the paramagnetic state, we obtain the expected hyperfine field of 13 kOe, which is in reasonable agreement with the experimental result. This indicates that the hyperfine interaction is dominated by the same mechanism for both the paramagnetic and the magnetically ordered states.

3.2.2. The zero-field spectrum. Figure 6 shows the zero-field spectrum of the low-temperature phase (1.4 K). The NQR line in the paramagnetic state (figure 1) is now separated into several lines due to the appearance of the hyperfine field. The lines are clearly resolved, which suggests that there exist only a few different Cu sites in this commensurate antiferromagnetic phase.

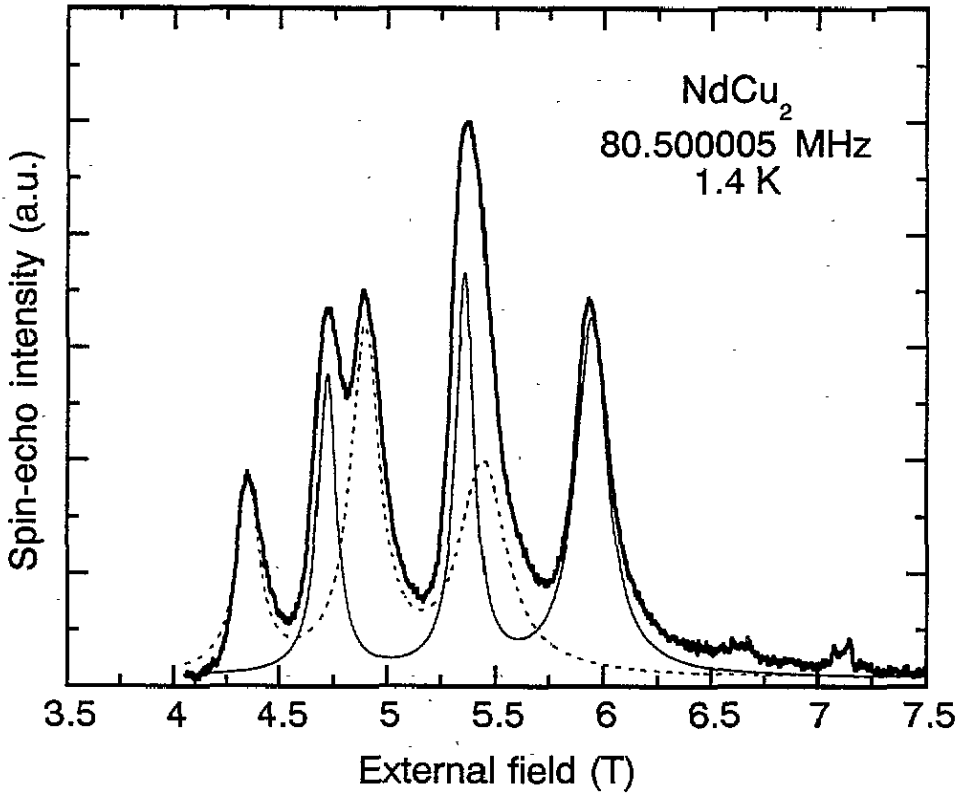

Figure 4. The field-swept NMR spectrum of $NdCu_2$ measured for a free powder sample (oriented as $H \parallel b$ axis) at 80.500 005 MHz and 1.4 K. Solid and broken curves indicate deconvoluted ^{63}Cu and ^{65}Cu resonances, respectively.

4. Discussion

The aim of the present investigation is to study the magnetic structure in the zero field below 1.4 K and to discuss the consistency between the NMR results and the magnetic structure as determined by neutron diffraction (Loewenhaupt *et al* 1995).

4.1. The model of the hyperfine field

First, a description of the internal field will be given. The Cu nucleus feels the transferred field from the ordered Nd moments. In a first approximation, we assume that the local field at the Cu site is given by

$$\boldsymbol{H}_{loc} = \boldsymbol{H}_{iso} + \boldsymbol{H}_{dip} \tag{6}$$

where the first term denotes the transferred hyperfine field which is assumed to be isotropic. This isotropic hyperfine field is caused either by the polarized conduction electron (RKKY interaction) or by an interaction due to the hybridization between f or d electrons of Nd and s or p electrons of Cu. The second term is the classical lattice dipole field produced by all Nd moments around the Cu nucleus.

In a first approximation, we consider only the field produced by the *effective* nearest-neighbour Nd atoms as $\boldsymbol{H}_{iso}$. The distances to these six *nearest-neighbour* Nd atoms are

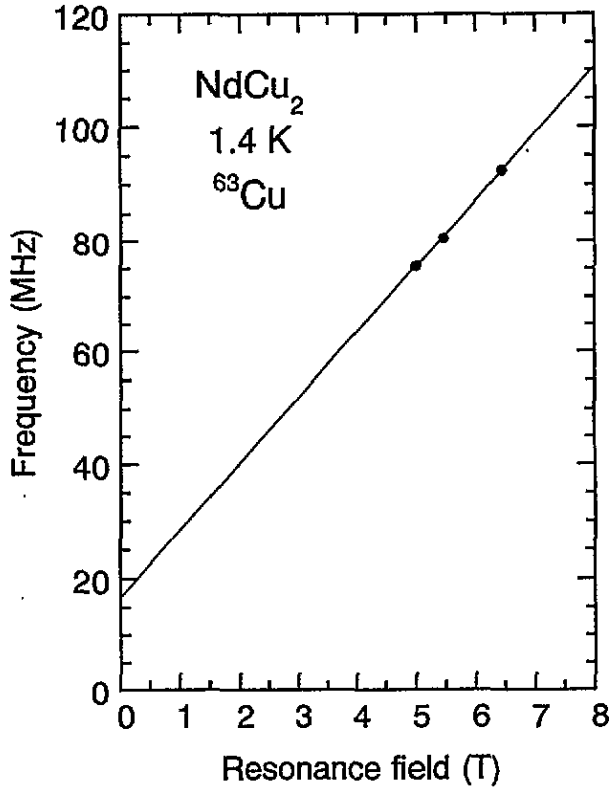

Figure 5. The frequency dependence of the ^{63}Cu resonance field of $NdCu_2$ in the ferromagnetic phase at 1.4 K. The typical error of the estimated resonance field is smaller than 0.01 T.

slightly different (see figure 8). Here, we calculate H_{iso} at the origin (Cu site) using the following equation:

$$H_{iso} = \alpha \sum_{i=1}^{6} \frac{\mu_i}{r_i^3} \tag{7}$$

where μ_i and r_i are the magnetic moment of the ith Nd atom and the distance between the Cu nucleus at the origin and the ith Nd atom, respectively, and α is a constant.

On the other hand, H_{dip} is given by

$$H_{dip} = \sum_{i}^{N} \left\{ \frac{3(\mu_i \cdot r_i) r_i}{r_i^5} - \frac{\mu_i}{r_i^3} \right\} \tag{8}$$

where r_i is the position of the ith Nd atom and the summation is taken over all the N Nd moments inside the considered volume.

4.2. Expected magnetic Cu sites in the low-temperature magnetic phase

From neutron diffraction measurements of a single crystal, Loewenhaupt *et al* (1995) found that the magnetic structure of the low-temperature phase can be described by a commensurate wave vector $\tau = (0.6, 0, 0)$ and its higher harmonics 3τ and 5τ, and that all Nd moments are oriented ferromagnetically along the b direction in each bc plane. Under this condition,

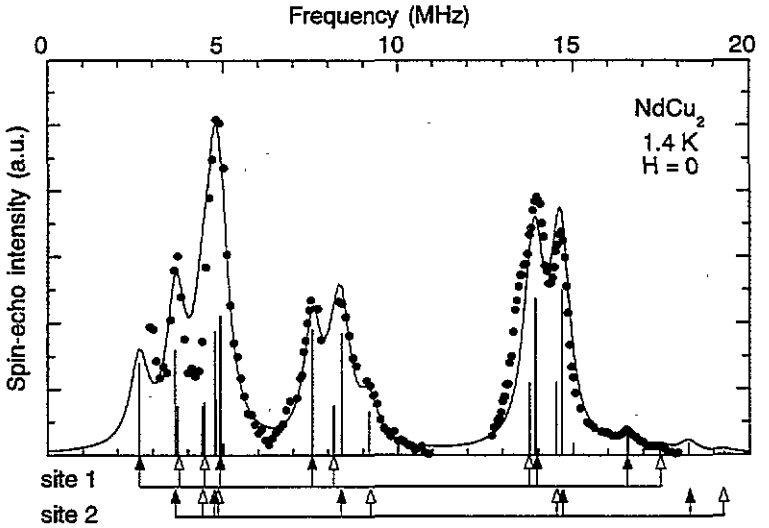

Figure 6. The zero-field ^{63}Cu and ^{65}Cu NMR spectrum of $NdCu_2$ at 1.4 K. Closed circles indicate experimental data measured at $\tau = 50$ μs (τ is the pulse separation of two spin echo pulses), which were divided by the square of the frequency. Positions of lines indicate the calculated resonance frequencies assuming two different magnetic Cu sites. Bold and fine lines represent the different sites. The lines indicated by closed and open arrows indicate the resonances of ^{63}Cu and ^{65}Cu, respectively. The heights of lines represent the expected intensity assuming a 1:1 population ratio for the two sites. A solid curve indicates the synthesized total intensity assuming a Lorentzian line with a full width at half maximum of 600 kHz for each resonance.

the description of the magnetic moment arrangement can be reduced to the one-dimensional problem with the period of $5a$ along the a direction, which has an Ising-like degree of freedom in the b direction. The moment of the ith layer in the a direction can be written as

$$\mu_i = \mu_\tau \sin(2\pi\tau R_i/a + \phi_1) + \mu_{3\tau} \sin(6\pi\tau R_i/a + \phi_2) + \mu_{5\tau} \sin(10\pi\tau R_i/a + \phi_3) \qquad (9)$$

where R_i are the positions of the ferromagnetic bc plane at $0, a/2, a, \ldots, 5a$ and ϕ_i are the phase angles. Using the values $\mu_\tau = 2.32\mu_B$, $\mu_{3\tau} = 0.90\mu_B$ and $\mu_{5\tau} = 0.36\mu_B$ and taking $\phi_1 = \phi_3 = \pi/2$ and $\phi_2 = -\pi/2$, Loewenhaupt *et al* (1995) proposed the magnetic structure shown in figure 7 with a unique moment of $\mu = 1.78\mu_B$ for all Nd atoms.

In this structure, all Cu sites within each bc plane are magnetically equivalent. Numbering each bc plane as shown in figure 7, we now can calculate the vector field describing the hyperfine coupling, $A_{iso}(= H_{iso}/\mu)$ and $A_{dip}(= H_{dip}/\mu)$, at each layer.

From the NMR results in the paramagnetic state, we concluded that the principal Z axis of the EFG is perpendicular to the a axis of the crystal; however, we could not determine the direction inside the bc plane. Here, we assume for simplicity that the Z axis is parallel to either the b or the c axis. As mentioned above, all the magnetic moments are oriented along the b direction. Therefore, we expect $\theta \sim 0°$ in the case b axis$\parallel$ Z axis and a large $\theta(\sim 90°)$ in the case c axis $\parallel$ Z axis, where θ is the angle between the hyperfine field direction and the Z axis. As will be mentioned below, it seems that the latter case is ruled out by the analysis of the zero-field spectrum. We therefore assume, in the following discussion, that the Z axis is parallel to the b axis of the crystal.

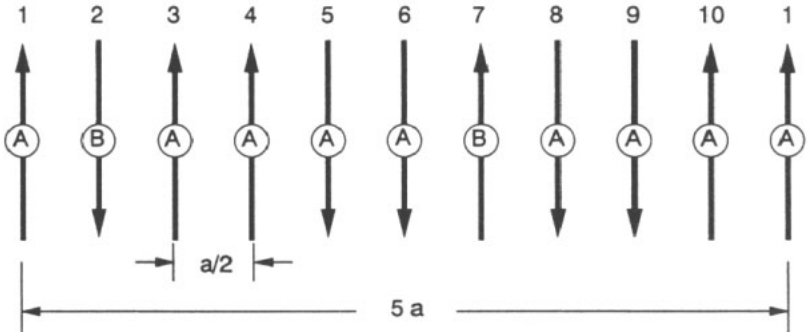

Figure 7. The magnetic structure of $NdCu_2$ in the low-temperature phase proposed by Loewenhaupt *et al* (1995). All Nd moments in each *bc* plane align ferromagnetically to the *b* direction. Each arrow represents the spin direction of the ferromagnetic *bc* plane. A and B represent different magnetic local symmetries of Cu on the corresponding plane (see figure 8).

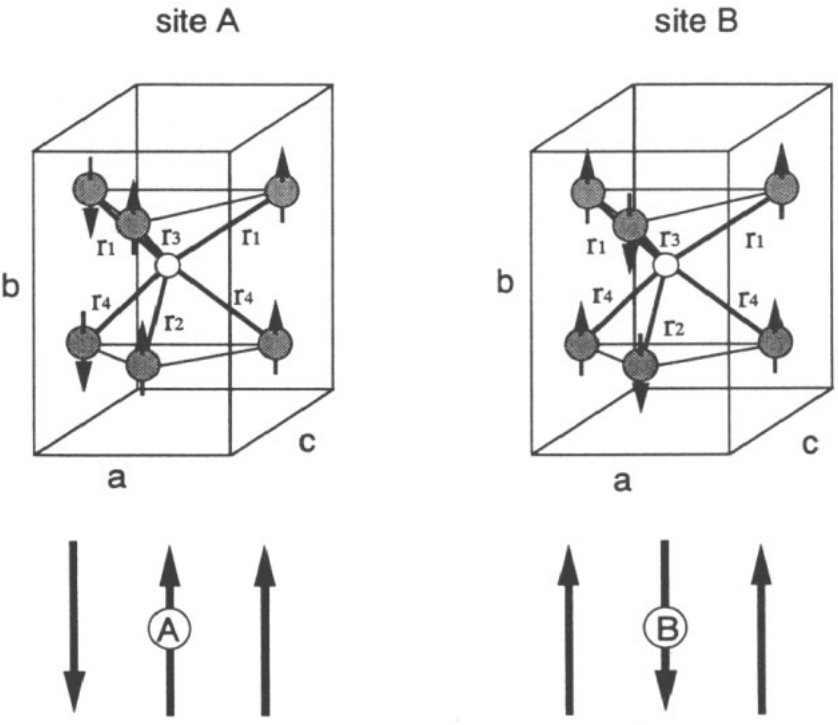

Figure 8. The local magnetic symmetry of the two different magnetic Cu sites, A and B. Open and hatched circles represents Cu and Nd atoms, respectively. Only effective nearest-neighbour magnetic atoms are shown. Arrows indicate the directions of Nd moments. Distances between central Cu and surrounding Nd atoms are slightly different: $r_1 = 3.01$ Å, $r_2 = 3.05$ Å, $r_3 = 3.10$ Å, $r_4 = 3.19$ Å (at room temperature). This difference gives rise to different values of the isotropic fields at sites A and B.

When considering the spin arrangement given by Loewenhaupt *et al* (1995) and taking into account only six effective nearest-neighbour Nd moments around the Cu site, we found

two types of magnetic local symmetry for the Cu atoms as shown in figure 8, denoted as A and B. The chemical Cu site is characterized by the combination of two tetrahedrons formed by a Cu atom and six Nd atoms. The magnitudes of the isotropic fields at sites A and B are slightly different because of the small differences among r_i. The angle θ should be 0° for both sites, reflecting the fact that the magnetic moments are parallel to the b axis.

Table 1. Calculated isotropic and dipole fields of Cu sites in the magnetic arrangement in figure 7

Position	A_{iso} (au)[a]	θ_{iso} (°)	A_{dip} (Oe μ_B^{-1})	θ_{dip} (°)	ϕ_{dip} (°)	Magnetic site
1	0.338	0	272	23.8	85.0	A
2	0.324	0	147	15.6	90.0	B
3	0.338	0	272	23.8	85.0	A
4	0.338	0	267	23.9	82.2	A
5	0.338	0	267	23.9	82.2	A
6	0.338	0	272	23.8	85.0	A
7	0.324	0	147	15.6	90.0	B
8	0.338	0	272	23.8	85.0	A
9	0.338	0	267	23.9	82.2	A
10	0.338	0	267	23.9	82.2	A

[a] The magnitude was taken to be unity in the case where all Nd moments align ferromagnetically along the b direction.

On the other hand, the dipole field is calculated over a sphere of 70 Å. The calculated field at the Cu site in each bc plane in figure 7 is listed in table 1 together with the relative values of the isotropic field. Here, the expected magnitude of the isotropic field in the case where magnetic moments align ferromagnetically along the b direction was taken to be unity. A_{dip} takes three different values but can be roughly classified into two groups. Therefore, as seen in table 1, the magnetic Cu sites can be recognized as two sites in the proposed magnetic structure. It should be noted that, in the magnetic structure shown in figure 7, the ratio of the numbers of these sites is 1:4.

4.3. The analysis of the zero-field spectrum

The analysis of the zero-field spectrum at 1.4 K is based on the nuclear spin Hamiltonian given by

$$[e^2qQ/4I(2I-1)][3I_Z^2 - I(I+1) + \tfrac{1}{2}\eta(I_+^2 + I_-^2)] - \gamma\hbar \boldsymbol{I}\cdot\boldsymbol{H} \qquad (10)$$

where the first and second terms are the quadrupole and the Zeeman terms, respectively. The eigenstates $|m\rangle$ and eigenvalues E_m obtained by solving the secular equation with the Hamiltonian (10) gives the resonance frequencies and the intensities as

$$h\nu(n \leftrightarrow m) = |E_n - E_m| \qquad (11)$$

$$I(n \leftrightarrow m) \propto |\langle n|I_x|m\rangle|^2. \qquad (12)$$

According to the suggested magnetic structure there should be two inequivalent Cu sites with different surroundings inside the magnetic unit cell. We therefore solved the secular equations for the two sites using the following adjustable parameters H, θ, ϕ, $\nu_Q(e^2qQ)$ and η.

Assuming that ν_Q and η are the same as those in the paramagnetic state ($^{63}\nu_Q$ = 8.86 MHz, η = 0.10), we tried to reproduce the experimental data. The resulting fit

procefure of the calculation to the experimental data is shown in figure 6. In this figure, the position of thin and bold straight lines represents the expected resonance frequencies for ^{63}Cu and ^{65}Cu, respectively, for each magnetic site. The reasonable agreement of the calculation with the experiment shows that our NMR experiment confirms the suggested *periodicity of the spin arrangement along the a direction*. This clearly shows that the Cu sites separates into two sites with different magnetic surroundings in this antiferromagnetic phase. For the fit procedure (figure 6), the following set of parameters were used:

$$H_1 = 5.25 \text{ kOe} \qquad \theta_1 = 20.5° \qquad \phi_1 = 90°$$
$$H_2 = 5.85 \text{ kOe} \qquad \theta_2 = 20.0° \qquad \phi_2 = 80°$$

where the suffix 1 or 2 denotes the different Cu sites. Using $\mu = 1.78\mu_B$/Nd obtained from single-crystal magnetization and neutron diffraction experiments, the hyperfine coupling constants for these two sites are

$$A_1 = 2.95 \text{ kOe } \mu_B^{-1} \qquad A_2 = 3.29 \text{ kOe } \mu_B^{-1}.$$

Because the calculated dipole field is of the order of 100 Oe μ_B^{-1} (see table 1), the isotropic contribution to the hyperfine field is dominant. In the paramagentic state, we estimated the hyperfine coupling constant $A = 7.34$ kOe μ_B^{-1}. Using equation (7) and referring to the relative values of the magnitude of the expected isotropic field (table 1), we expect that the hyperfine coupling constant is reduced to about 2.5 kOe μ_B^{-1} in the antiferromagnetic state. This is in reasonable agreement with the above experimental values, suggesting the same hyperfine mechanism for all the paramagnetic, ferromagnetic and antiferromagnetic states. Assuming that the hyperfine interaction can be described as in subsection 4.1, we expect small θ values if the Nd moments are pointing along the b direction. Therefore, the small values of obtained θ justify the assumption that the Z axis is parallel to the b axis of the crystal, and a small tilt from the b axis is ascribed to the dipole field.

The integrated intensity of the resonance from a certain site should be proportional to the number of atoms which belong to the sites. In fact, in figure 6, the height of lines represents the expected intensity assuming a 1:1 population ratio for the two sites. A solid curve indicates the synthesized total intensity assuming a Lorentzian line with a constant width for each resonance. The experimental intensities measured at a constant τ (τ is the pulse separation of two spin echo pulses), shown by closed circles, were divided by the square of frequency as usually done for an antiferromagnet in order to correct the frequency dependence of the Boltzmann factor for the equilibrium nuclear magnetization and of the signal voltage induced in the coil. It seems that the experimental result is, *accidentally*, in fairly good agreement with the calculation in spite of the fact that a 1:4 population ratio is anticipated for the spin arrangement in figure 7. The origin of this discrepancy is not clear but may be explained as follows. Usually, in discussing the frequency dependence of the signal intensity, the frequency dependence of the spin echo decay time, T_2, should be taken into account. We have measured spin echo decay curves at several frequencies and found the frequency dependence to be small. However, the shape of the curves is not single exponential but multiexponential, suggesting that T_2 is not the same for all nuclei. This fact makes the T_2 correction of the intensity difficult. Naively, the spin–spin relaxation rate is proportional to the probability of finding like nuclei which feel the same hyperfine field. This implies that T_2 of the major site is smaller than that of the minor site, i.e. the intensity of the major site is more reduced at a finite τ. This is one of the reasonable explanations of the discrepancy between experiment and calculation, although we feel that the discrepancy is too large to be explained by only this effect.

5. Conclusion

In order to obtain information on the magnetic structure of $NdCu_2$ in the low-temperature commensurate phase, we measured Cu NMR in both paramagnetic and magnetically ordered states. It was found that the structural Cu site in the paramagnetic state separates into two sites with different magnetic surroundings below 4.1 K in this commensurate antiferromagnetic state. This observation is in agreement with the magnetic structure proposed by Loewenhaupt *et al* (1995) for the magnetic state below 4.1 K.

Acknowledgments

We would like to thank Dr M Loewenhaupt for very valuable discussions. Two of the authors (HT and HN) would like to acknowledge useful discussions with Dr S Kawarazaki and much technical support by Mr R Iehara.

References

Arons R R, Loewenhaupt M, Reif Th and Gratz E 1994 *J. Phys.: Condens. Matter* **6** 6789

Bozukov L, Gilewski A, Gratz E, Apostolov A and Kamenov K 1992 *Physica* B **177** 299

Gratz E, Loewenhaupt M, Divis M, Steiner W, Bauer E, Pillmayr N, Müller H, Nowotny H and Frick B 1991 *J. Phys.: Condens. Matter* **3** 9297

Gratz E, Rotter M, Lindbaum A, Müller H, Bauer E and Kirchmayr H 1993 *J. Phys.: Condens. Matter* **5** 567

Hashimoto Y, Fujii H, Fujiwara H and Okamoto T 1979 *J. Phys. Soc. Japan* **47** 73

Lebech B, Smetana Z and Sima V 1987 *J. Magn. Magn. Mater.* **70** 97

Loewenhaupt M, Reif Th, Arons R R, Gratz E, Rotter M and Lebech B 1995 *Z. Phys.* B **96** 491

Sherwood R C, Williams H J and Wernick J H 1964 *J. Appl. Phys.* **35** 1049

Svoboda P, Divis M, Andreev A V, Baranov N V, Bartashevich M I and Markin P E 1992 *J. Magn. Magn. Mater.* **104–107** 1329